Supplemental Data

Table S1. Inter-subunit DEER distances from the cdb3 homo-dimer between two identical sites on the peripheral domains of each cdb3 subunit.

For three sites on the peripheral domains of cdb3, DEER distances were measured in the absence and then in the presence of AnkD34. The mean distances and their distributions (numbers in parentheses) are shown below along with the corresponding Cβ-Cβ distances from the crystal structure.

Spin labeled sites on cdb3	Distance (Å)		Cβ-Cβ distance (Å) in crystal structure
	- AnkD34	+ AnkD34	
84	26.1 (0.4)	26.2 (0.3)	23.9
302	56.5 (0.2)	57.2 (6.8)	53.8
340	34.6 (0.8)	33.5 (0.5)	30.4

Table S2. Intra-protein DEER distances from both the concave groove and the convex backbone sides of AnkD34.

For a set of doubly labeled mutants of AnkD34, DEER distances were measured in the absence and then in the presence of cdb3. The mean distances and their distance distributions (numbers in parentheses in Å) are shown below along with the corresponding Cβ-Cβ distances from the crystal structure.

Spin-labeled sites		Distance (Å)		Cβ-Cβ distance (Å) in crystal structure
		- cdb3	+ cdb3	
Concave groove (Inner helices)	410/509	24.4 (2.7)	24.3 (3.0)	25.1
	509/608	22.1 (2.2)	22.0 (1.9)	26.2
	608/707	22.3 (2.3)	21.9 (2.0)	25.0
Convex backbone (Outer helices)	425/524	41.5 (8.6)	41.3 (6.8)	34.8
	524/623	35.3 (4.0)	32.0 (6.4)	33.9
	623/722	40.3 (1.5)	39.7 (2.3)	36.2
	722/788	30.7 (3.7)	30.6 (3.9)	25.5

Fig. S1. Dipolar coupled EPR spectra obtained from the sites at the dimer interface of cdb3 in the presence or absence of AnkD34

The DEER data in Fig. 2 of the manuscript indicate that there are not any significant global structural changes in the cdb3 dimer upon complex formation with AnkD34. This result was further confirmed by careful characterization of any potential structural changes in the dimer interface as shown by the EPR data in Fig. S1 (black, without AnkD34; red, with AnkD34). Sites 105, 108, 112, and 339 are all at the dimer interface and each give rise to a dipolar coupled EPR spectrum due to their close proximity. These spectra, which are extremely sensitive to changes in the average inter-probe distance and their relative orientations, show conclusively that binding of wt-AnkD34 to the peripheral domain of each monomer of cdb3 does not lead to any observable changes in the structure of the dimer interface.

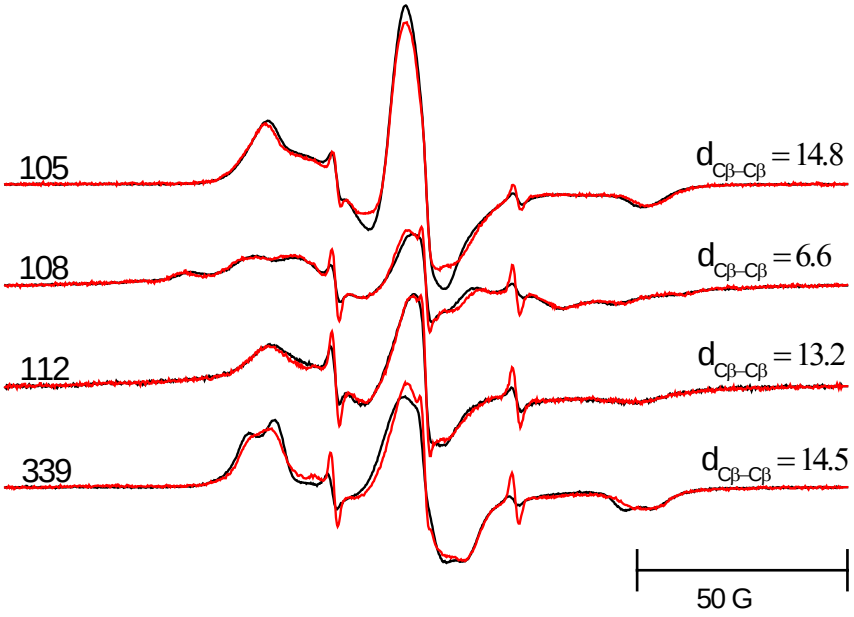

Fig. S2. The effect of mutation and spin labeling at various sites of cdb3 on its binding affinity for AnkD34.

Relative binding affinities for selected spin labeled mutants of cdb3 with wt-AnkD34 were measured by the pull down assay as described in the experimental procedures section of the manuscript. The relative affinities of 26 sites are compared with binding of wt-cdb3 to wt-AnkD34 in panel B (bottom) of Figure S2. It was observed that most of the sites showed binding that was >80% of that observed with wt-cdb3. However, introduction of a single cysteine and spin labeling at sites 70, 72, 129, 155, and 158 all resulted in a reduction in relative binding affinity to <40% of the value for wt-cdb3. It is concluded that each of these sites on the peripheral domain of cdb3 must result in unfavorable steric and/or electrostatic interactions at the cdb3-AnkD34 interface and therefore, must lie at, or near, the interacting surface of cdb3. The SDS-PAGE gel in the panel A (top) demonstrates the pull down assay results for sites 70, 72, 126, 158, 159, 160, 166, 252, and 254

.

A

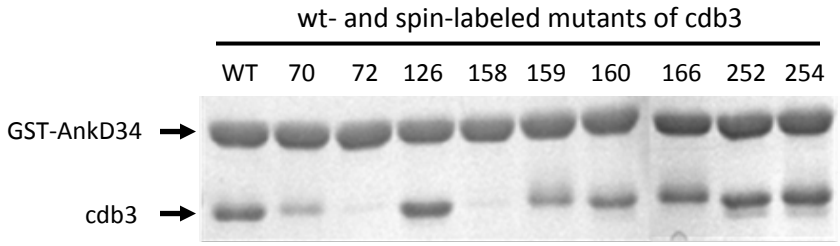

B

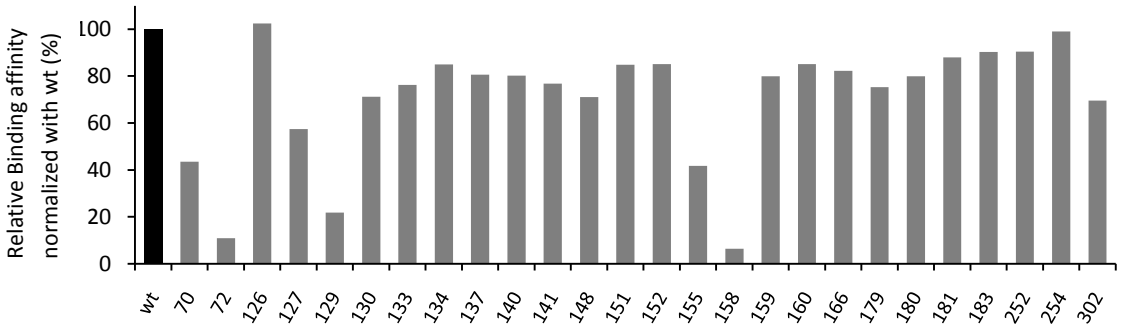

Fig. S3. The effect of mutation and spin labeling at various sites of AnkD34 on its binding affinity for cdb3.

Relative binding affinities for selected spin labeled mutants of AnkD34 with wt-cdb3 were also measured by the pull down assay as described in the experimental procedures section of the manuscript. The relative affinities of 6 sites are compared with binding of wt-AnkD34 to wt-cdb3 in the panel B (bottom) of Fig. S3. Spin labeling at sites 598 on ankyrin repeat 18, 631 on ankyrin repeat 19, and sites 652 and 664 on ankyrin repeat 20 all resulted in relative binding affinities that were >70% of that observed with wt-AnkD34. However, labeling at sites 596 in ankyrin repeat 18 and at site 629 in ankyrin repeat 19 resulted in less than 20% of the binding relative to wt-AnkD34. The SDS-PAGE gel in panel A (top) demonstrates the dramatic reduction in relative binding affinity for sites 596 and 629 again indicating that spin labeling at these sites result in unfavorable steric and/or electrostatic interactions at the binding interface. The results presented in Figs. S2 and S3 provide additional information for evaluating the model for the complex between cdb3 and AnkD34 as described in the manuscript.

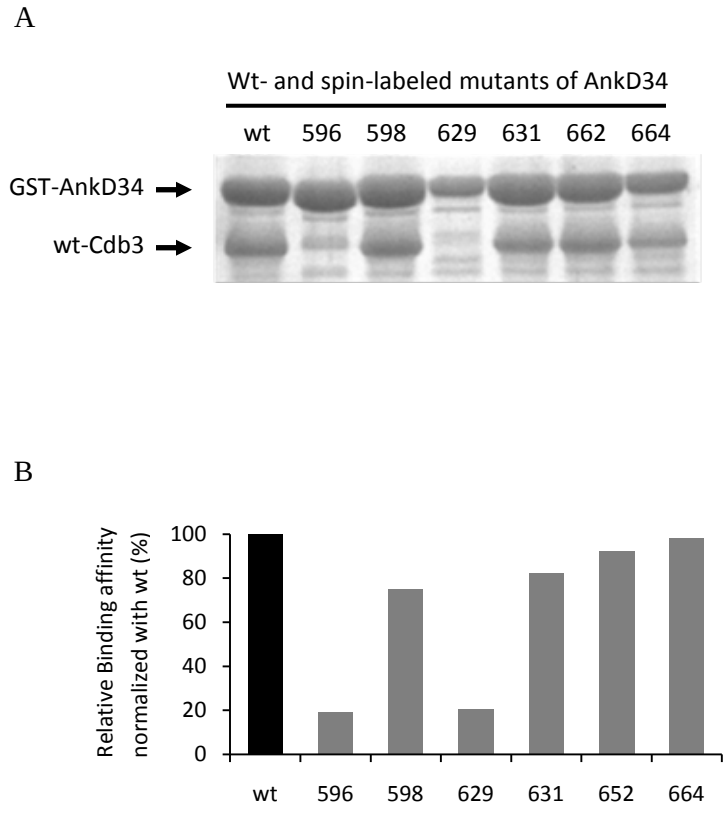

Fig. S4. DEER data and the resultant distance distributions for the remaining 17 interprotein distance constraints which were employed to construct the model for the complex.

A total of 20 inter-protein distance constraints between spin labeled sites on cdb3 and on AnkD34 were obtained from DEER measurements as defined in Fig. 8 in the manuscript. The experimental DEER data and analyses from three of the inter-protein measurements (133cdb3/608AnkD34; 166cdb3/707AnkD34; and 254cdb3/616AnkD34) were also included in Fig. 8. Fig. S4 shows the DEER data and analyses (inset, distance distributions in Å) for the remaining 17 sites (labeled as 'cdb3:AnkD34' in each plot) that were used to construct the model for the complex shown in Fig. 10 of the manuscript. The results of the analyses from all pairs of sites are tabulated in Table 3 of the manuscript. Some of the DEER data showed the presence of the second long distance component which originated from the relatively short (< 60Å) cdb3 intra-dimer distances and they are marked with red arrows in this figure.

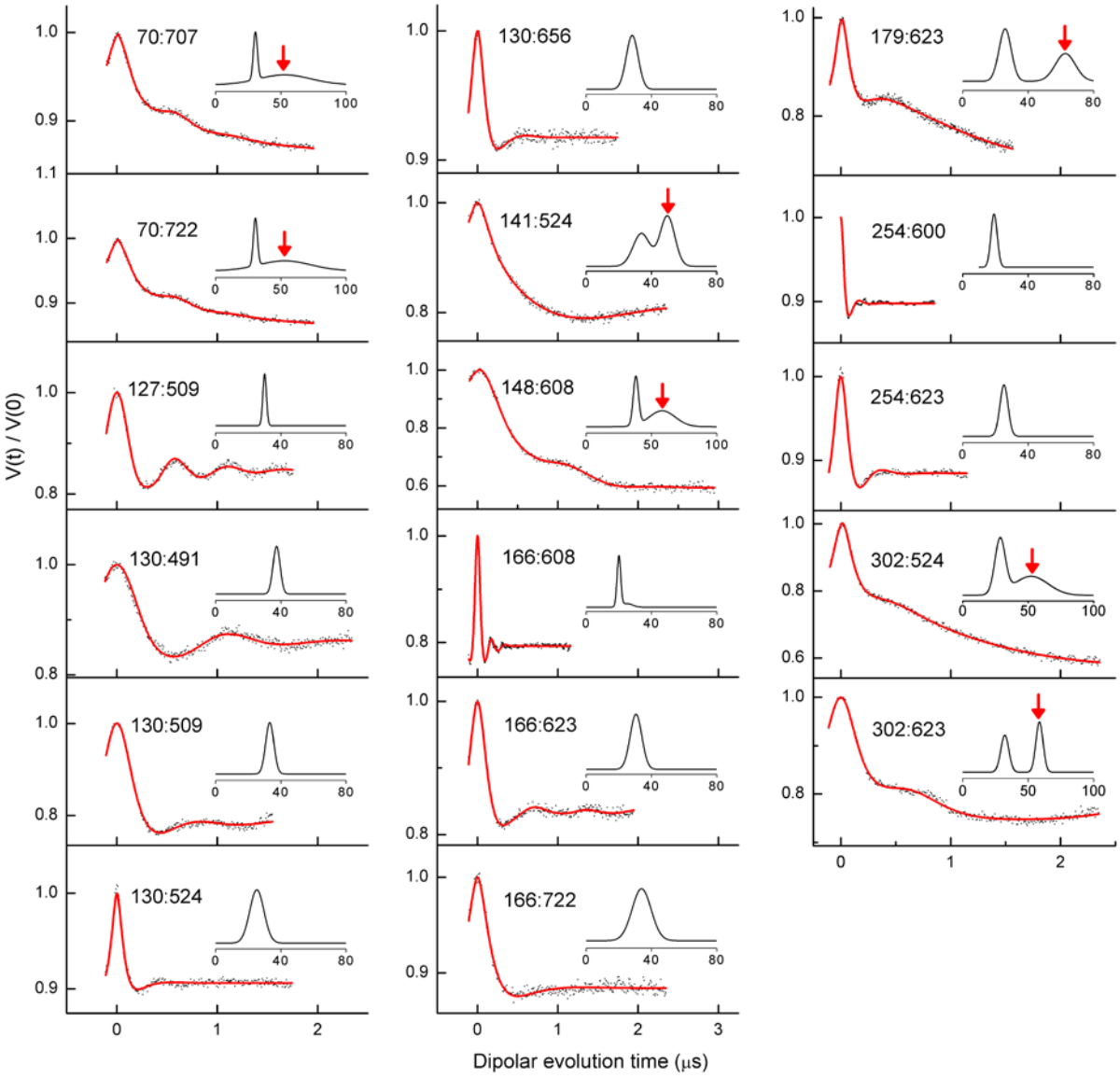

Fig. S5. Exchange and dipolar coulpling from pairs of labeled sites near the binding interface.

The data in Fig. 12 in the manuscript show strong dipolar and exchange coupling between spin label pairs 133cdb3/590AnkD34, 151cdb3/623AnkD34, and 181cdb3/656AnkD34, all of which are predicted by the structural model in Fig. 10 to be at the binding interface between the two proteins. The models in Fig. 10 in the manuscript and in more detail, in panel B, which presents one of those models with measured distances, also predicts close proximity between 133cdb3/623AnkD34, between 151cdb3/590AnkD34, and between 151cdb3/656AnkD34. However, it predicts much weaker interactions between 133cdb3/656AnkD34, between 181cdb3/590AnkD34, and between 181cdb3/623AnkD34. The additional 6 EPR spectra shown in Fig. S5 confirm these predictions. Each EPR spectrum obtained from the complexes (red) was compared with that from the corresponding sum of single spin labeled constructs (black).

A

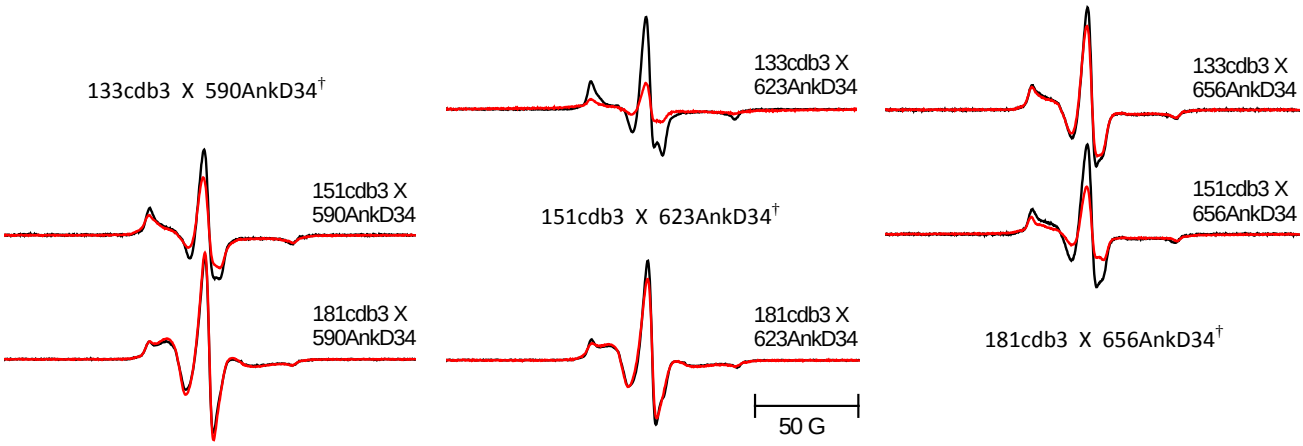

†, EPR spectra are in Fig. 11 in the manuscript and their corresponding distances were highlighted with red dashed lines in panel B.

B